Polyvalent Cations Constitute the Voltage Gating Particle in Human Connexin37 Hemichannels

Michael C. Puljung,[1] Viviana M. Berthoud,[2] Eric C. Beyer,[2] and Dorothy A. Hanck[3]

[1]Department of Neurobiology, Pharmacology, and Physiology, [2]Department of Pediatrics, and [3]Department of Medicine, The University of Chicago, Chicago, IL 60637

ABSTRACT Connexins oligomerize to form intercellular channels that gate in response to voltage and chemical agents such as divalent cations. Historically, these are believed to be two independent processes. Here, data for human connexin37 (hCx37) hemichannels indicate that voltage gating can be explained as block/unblock without the necessity for an independent voltage gate. hCx37 hemichannels closed at negative potentials and opened in a time-dependent fashion at positive potentials. In the absence of polyvalent cations, however, the channels were open at relatively negative potentials, passing current linearly with respect to voltage. Current at negative potentials could be inhibited in a concentration-dependent manner by the addition of polyvalent cations to the bathing solution. Inhibition could be explained as voltage-dependent block of hCx37, with the field acting directly on polyvalent cations, driving them through the pore to an intracellular site. At positive potentials, in the presence of polyvalent cations, the field favored polyvalent efflux from the intracellular blocking site, allowing current flow. The rate of appearance of current depended on the species and valence of the polyvalent cation in the bathing solution. The rate of current decay upon repolarization depended on the concentration of polyvalent cations in the bathing solution, consistent with deactivation by polyvalent block, and was rapid (time constants of tens of milliseconds), implying a high local concentration of polyvalents in or near the channel pore. Sustained depolarization slowed deactivation in a flux-dependent, voltage- and time-independent fashion. The model for hCx37 voltage gating as polyvalent block/unblock can be expanded to account for observations in the literature regarding hCx37 gap junction channel behavior.

KEY WORDS: gap junction • gating mechanism • divalent cation • chemical gating • voltage-dependent block

INTRODUCTION

In vertebrate cells, direct cytoplasmic coupling is achieved through gap junction channels. These channels, oligomers of connexin proteins, are permeable to a wide variety of ions, nutrients, and second messenger molecules as large as 1 kD (Schwarzmann et al., 1981; Imanaga et al., 1987). Within a cell, connexins assemble to form hexameric connexons or hemichannels, with the subunits arranged symmetrically around a large, central pore. Once in the plasma membrane, hemichannels dock with connexin hemichannels in the plasma membranes of closely apposed cells to form dodecameric gap junction channels (for review see Saez et al., 2003). Connexin hemichannels must exist at least transiently in the plasma membrane of cells before they pair with another connexon to form a gap junction channel. Given that hemichannels have large single channel conductances and are permeable to large solutes, it is imperative that their opening be tightly regulated, i.e., hemichannels must be closed when they are unpaired, but open when they are paired so that cytoplasmic coupling may be achieved.

There are many ways in which opening of connexin channels is regulated. Gating of gap junctions by the action of Ca^{2+} has been established for decades (for review see Peracchia, 2004). More recent reports also suggest a role for Mg^{2+} (Ramanan et al., 1999; Banach et al., 2000; Ebihara et al., 2003) as well as polyamines (Musa and Veenstra, 2003) in connexin channel gating. One feature common to all vertebrate gap junctions studied under voltage clamp is sensitivity to the transjunctional voltage difference between two coupled cells (for review see Harris, 2001). If two coupled cells are isopotential, the gap junctional conductance is maximal. Upon depolarization or hyperpolarization of one cell relative to the other, conductance initially remains the same, but over time decreases to a smaller, steady-state value. Unpaired connexin hemichannels also are gated by voltage, typically opening only upon depolarization (e.g., Ebihara and Steiner, 1993; Gupta et al., 1994; Pfahnl et al., 1997; Gomez-Hernandez et al., 2003). This process is not completely understood, since no putative voltage sensing region, like the canonical S4

Address correspondence to Michael Puljung, 5841 South Maryland Ave., MC6094, Chicago, IL 60637. Fax: (773) 702-6789; email: mpuljung@uchicago.edu

Abbreviation used in this paper: hCx37, human connexin37.

segments of voltage-gated cation channels, is present in any of the 20 human connexin sequences identified. Mutations in disparate regions including the cytoplasmic NH_2 (Kumari et al., 2000; Oh et al., 2000; Purnick et al., 2000b) and COOH termini (Revilla et al., 1999; Anumonwo et al., 2001) as well as in extracellular loop regions important for docking between hemichannels (Oh et al., 2000) and pore lining residues (Kumari et al., 2001) have all been shown to affect the voltage sensitivity of the junctional conductance. Furthermore, many gap junction proteins such as human connexin37 (hCx37), the focus of this study, are expressed in nonexcitable tissues, where they are unlikely to experience a transjunctional voltage gradient under physiological conditions.

We report here the formation of functional hCx37 hemichannels, exogenously expressed in *Xenopus laevis* oocytes. hCx37 hemichannels were sensitive to voltage, closing at potentials negative to +40 mV. Polyvalent cations were required for channel closure and affected the activation kinetics at positive potentials. We propose a model for connexin hemichannel gating based on voltage-dependent block of the channels by polyvalent cations. This model, which combines the previously studied aspects of divalent cation and voltage gating into a common process, in which voltage gating arises from electrostatic modulation of polyvalent cation binding sites that are located on the cytoplasmic side of the voltage field, is sufficient to account for a wide range of hemichannel behavior and hCx37 gap junction channel gating observations in the literature. The model derives from elements of voltage-dependent block first characterized in narrow pores in which block is complete and rapid, modified to account for the fact that, in large pores like those of hCx37 hemichannels, block may involve multiple sites, can be quite slow or fast depending on experimental conditions, and that the ions involved not only block, but permeate. Some of the data have been presented in abstract form (Puljung et al., 2000, 2001a,b, 2003).

MATERIALS AND METHODS

RNA Preparation

The cDNA encoding human connexin37 (hCx37), flanked by the 5′ and 3′ untranslated regions of the *Xenopus* globin gene was subcloned into the Bluescript SK vector (Stratagene). The template was linearized with XbaI and transcribed according to the manufacturer's protocol using the T7 mMessage mMachine Kit (Ambion). Transcripts were diluted in RNase-free TE, pH 8.0.

Oocyte Preparation

Stage V and VI oocytes were isolated from adult female *Xenopus laevis* frogs under tricaine anesthesia, treated with collagenase (1–2 mg/ml for 2× 50 min) in $0Ca^{2+}$OR2 (90 mM NaCl, 2.5 mM KCl, 1 mM $MgCl_2$, and 5 mM HEPES, pH 7.6), and manually defolliculated in OR2+ (90 mM NaCl, 2.5 mM KCl, 1 mM $MgCl_2$, 1 mM $CaCl_2$, 0.27 g/L pyruvic acid sodium salt, 2 mg/L gentamicin, and 5 mM HEPES, pH 7.6). Oocytes were injected with a total volume of 50 nL, 25 nL corresponding to the diluted RNA transcript (or RNase-free TE, pH 8.0, for control oocytes), and 25 nL of a 0.30 ng/nL (in RNase-free TE, pH 8.0) solution of an antisense oligonucleotide directed against the endogenous *Xenopus* Cx38 protein (AntiCx38) expressed in oocytes (Barrio et al., 1991). Oocytes were injected in OR2+ and stored in 0DivOR2 (90 mM NaCl, 2.5 mM KCl, and 5 mM HEPES, pH 7.6) for at least 8 h following injection before recording. Procedures were performed in accordance with an IACUC-approved protocol.

Oocyte Electrophysiology

Electrophysiological recordings on oocytes were performed using the two-microelectrode voltage clamp method in 0DivOR2. Additions to this solution are indicated in the figure legends. Solution exchange was achieved using a gravity perfusion system. Exchange of the bath solution occurred with a time constant of ~24 s, as assayed by examining the rate of disappearance of exogenously expressed Na^+ current when exchanging OR2+ solution for one in which the Na^+ was replaced with Cs^+ (not depicted). Pipettes were pulled to a resistance of 0.3 MΩ to 2.0 MΩ and filled with a solution containing 3 M KCl. Recordings were performed using a Dagan CA1-B oocyte clamp (Dagan Corporation). Signals were filtered at 1 kHz and digitized with a Digidata 1200 analogue/digital converter (Axon Instruments, Inc.) at 2 kHz, unless otherwise noted, using pClamp 8 (Axon Instruments, Inc.). All experiments were performed at room temperature (20–24°C). Time course experiments were performed by sampling the holding current at a given potential for a period of 100 ms, once per second.

Data Treatment and Analysis

Peak current for the isochronal current–voltage protocols was measured between 2,383 and 2,433 ms after the initiation of the voltage pulse. For raw current traces presented in the figures, only every 100th point is plotted. No capacitance correction was used. Leak correction, when applied, was performed either by extrapolating from linear regression to data at negative potentials or by assuming a line between the current at the holding potential and the origin unless otherwise indicated. Data analysis was performed using MATLAB version 6.5 (The Math Works, Inc.) and Microcal Origin version 7 (OriginLab Corporation). Group statistics are reported as mean ± SEM.

Concentration Responses

Divalent cations were washed in at −40 mV. To better appreciate the amount of current blocked during the wash-in, the peak current from 2.5-s pulses to −80 mV, where currents were larger due to an increased driving force, was measured and plotted as a function of divalent cation concentration. The binding of polyvalent cations was so slow that no appreciable change in the fraction of block occurred during the time the potential was changed to −80 mV. Block was assumed to be complete in 2 mM Ca^{2+} and absent in 20 μM Ca^{2+}. Mg^{2+} data were normalized to the Ca^{2+} data by applying a saturating concentration of Ca^{2+} (2 mM) to the oocytes following wash-in of Mg^{2+}. The concentration–response relationships were fit with Langmuir isotherms of the form $\%\text{Block} = A/(1 + 10^{(\log(IC50) - [M])p})$, where A is maximum response (normalized to 1 for Ca^{2+}), IC_{50} is the half-maximal inhibitory concentration, [M] is the concentration of the metal ion, and p is the Hill coefficient.

Chemicals and Supplies

Standard solutions of $MgCl_2$ and $CaCl_2$ were obtained from Fluka. All other chemicals were obtained from Sigma-Aldrich.

RESULTS

hCx37 Hemichannel Currents in Xenopus Oocytes

Previously, only intercellular channels in dual whole-cell or dual oocyte recordings of connexin37 have been reported (Willecke et al., 1991; Reed et al., 1993; Traub et al., 1998; Ramanan et al., 1999; Banach et al., 2000). We find that, when RNA transcript for hCx37 was injected into *Xenopus laevis* oocytes along with an antisense oligonucleotide (AntiCx38) directed against the expression of endogenous *Xenopus* connexin38, currents could be measured from functional hCx37 hemichannels in unapposed oocyte membranes. Fig. 1 A (top) shows currents recorded in 0DivOR2 (see MATERIALS AND METHODS) plus 1 mM Ca^{2+}. Under these ionic conditions, hCx37 hemichannel currents resembled previously recorded hemichannel currents generated by Cx46, Cx44, Cx56, Cx38, $Cx32E_1$43, Cx50, Cx45, and Cx32 (Paul et al., 1991; Ebihara and Steiner, 1993; Gupta et al., 1994; Ebihara et al., 1995; Ebihara, 1996; Pfahnl et al., 1997; Beahm and Hall, 2002; Valiunas, 2002; Gomez-Hernandez et al., 2003). Channels opened upon depolarization, and currents increased throughout the duration of the depolarizations. However, under these conditions, the hCx37 hemichannel currents were contaminated by a slow Na^+ current, which is endogenously expressed in *Xenopus* oocytes (Kado and Baud, 1981; Baud et al., 1982; Baud and Kado, 1984; Ripps et al., 2002a,b). Fig. 1 A (bottom) shows an example of these currents from a control oocyte injected only with AntiCx38, recorded in 0DivOR2 plus 1 mM Ca^{2+}, and Fig. 1 B shows an average current–voltage relationship for oocytes injected with AntiCx38 (circles) and recorded in 0DivOR2 containing 0.5 mM Ca^{2+}. The current–voltage relationship is characteristic of the endogenous oocyte Na^+ current in that activation occurred at potentials positive to +20 mV, and currents reversed at ~+90 mV, near the predicted value for E_{Na}, assuming an intracellular Na^+ concentration of 2.5 mM. Fig. 1 B (squares) corresponds to the average current–voltage relationship for oocytes injected with hCx37 RNA plus AntiCx38, recorded in 0DivOR2 plus 0.5 mM Ca^{2+}. Fig. 1 C (squares) shows an average current–voltage relationship for hCx37, with currents normalized to the peak current measured at +90 mV, corrected by the mean of the current in control oocytes, i.e., those injected only with AntiCx38. Activation of hCx37 hemichannels occurred at potentials positive to +30 mV.

To verify that these currents represented functional hCx37 hemichannels, a commonly used gap junction channel blocker, 1-heptanol, was added to the bathing medium of 0DivOR2 plus 0.5 mM Ca^{2+}. Addition of 10 mM 1-heptanol to control oocytes completely inhibited the endogenous Na^+ current (unpublished data) and 67% of the outward current in hCx37-injected oocytes (Fig. 1 C, circles). These data support the idea that currents were the result of expression of hCx37 as functional hemichannels.

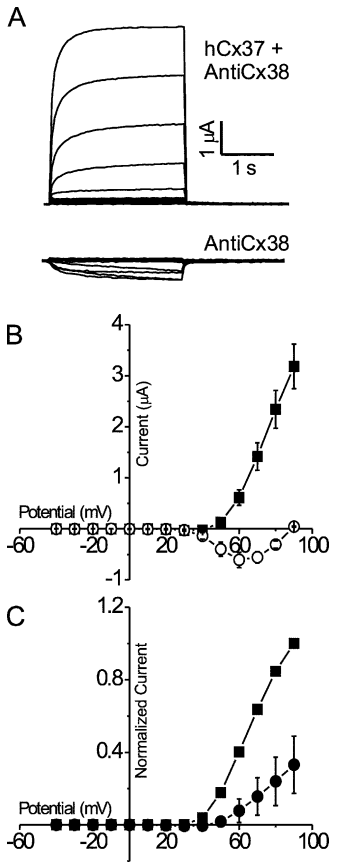

FIGURE 1. Nonjunctional currents from hCx37 expressed in *Xenopus laevis* oocytes. (A, top) Currents resulting from a series of voltage steps from a holding potential of −40 mV in 10-mV increments to a potential of +90 mV in an oocyte injected with RNA encoding hCx37 plus AntiCx38. (A, bottom) Currents from an oocyte injected only with AntiCx38. Currents were recorded in 0DivOR2 plus 1 mM Ca^{2+}. (B) Average, isochronal (see MATERIALS AND METHODS) current–voltage relationship for oocytes injected with hCx37 RNA plus AntiCx38 (■, n = 10) and oocytes injected only with AntiCx38 (○, n = 3). Currents were recorded in 0DivOR2 plus 0.5 mM Ca^{2+}. (C) Normalized, average, isochronal current–voltage relationships for oocytes injected with hCx37 RNA plus AntiCx38, recorded in 0DivOR2 plus 0.5 mM Ca^{2+} in the presence (●, n = 3) or absence (■, n = 10) of 10 mM 1-heptanol. Currents in the absence of heptanol were corrected by subtracting the mean of the oocytes injected only with AntiCx38. Currents in the presence of heptanol were not corrected by the control currents, since the endogenous sodium current in oocytes was completely inhibited by 10 mM 1-heptanol (not depicted). All currents were normalized to the peak current at +90 mV in the absence of 1-heptanol. The current–voltage relationships were all leak corrected.

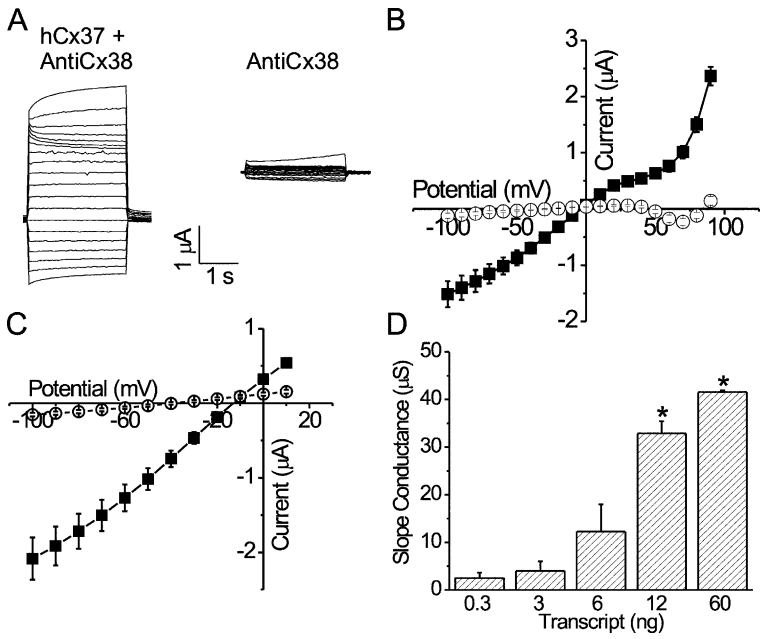

FIGURE 2. hCx37 hemichannel currents lose their voltage and time-dependent properties in oocytes following wash-out of divalent cations. (A) Representative currents resulting from a series of steps from a holding potential of −40 mV to potentials ranging from −100 to +90 mV in 10-mV increments for an oocyte injected with hCx37 RNA along with AntiCx38 (left) and an oocyte injected with AntiCx38 alone (right) stored in 0DivOR2. (B) Average, isochronal current–voltage relationships over the voltage range from −100 to +90 mV for oocytes injected with hCx37 RNA plus AntiCx38 (■, $n = 6$) and oocytes injected only with AntiCx38 (○, $n = 5$). (C) Average, isochronal current–voltage relationships over the voltage range from −100 to +10 mV for oocytes injected with hCx37 RNA plus AntiCx38 (■, $n = 30$) and oocytes injected only with AntiCx38 (○, $n = 20$). (D) Bar graph showing macroscopic hCx37 hemichannel conductance (assessed between −60 and 0 mV) as a function of the amount of hCx37 RNA injected into the oocyte ($n = 2$, 60 ng; $n = 3$, 12 ng; $n = 4$, 6 ng; $n = 4$, 3 ng; $n = 4$, 0.3 ng). The asterisk corresponds to current levels that were significantly larger than those with 0.3 ng injected ($P < 0.0001$, Student's *t* test).

Depletion of Divalent Cations Results in Loss of Gating at Negative Potentials

When oocytes expressing hCx37 were voltage clamped in a solution containing no divalent cations (0DivOR2), currents were quite different. In the absence of divalent cations, hCx37 hemichannels were not closed at potentials negative to +40 mV, but rather passed current linearly with respect to voltage (Fig. 2 A, left). At potentials positive to +10 mV, the presence of the endogenous Na^+ current (Fig. 2 B) produced a deviation from linearity in the current. Current–voltage data from oocytes expressing hCx37 are summarized in Fig. 2 B (squares). We first focused on the range of potentials where there was no hemichannel current in the presence of divalent cations. Current over this range remained at approximately the same level for the duration of the voltage pulse (Fig. 2 A, left). In the absence of divalent cations, oocytes injected only with AntiCx38 also produced currents that were linear with respect to voltage over this range, but were much smaller than the hCx37 currents (Fig. 2 A, right). The reversal potential of the endogenous oocyte currents was −40 mV (Fig. 2 C, circles), which represented a high, background permeability to either Cl^- or K^+ in *Xenopus* oocytes, which are known to express channels selective for both ions (Weber, 1999).

The presence of both inward and outward currents (Fig. 2 C, squares) allowed for the appreciation of the reversal potential for hCx37 hemichannels which, under these conditions, was −13 mV, an expected value for a weakly selective channel like hCx37 (Veenstra et al., 1994), and similar to the value of −9.3 mV measured for Cx46 hemichannels (Ebihara and Steiner, 1993). Importantly, this reversal potential was not zero, which is the reversal potential expected for a linear leak. To provide further support that these currents were due to hCx37 hemichannels open at potentials negative to the activation threshold in the presence of Ca^{2+}, and not leak, currents were measured from oocytes injected with increasing amounts of hCx37 RNA. The data shown in Fig. 2 D illustrate that slope conductance between −60 and 0 mV increased when increasing amounts of hCx37 RNA were injected into oocytes. The same volume was used to inject each oocyte, so the increase in conductance was not the result of opening of stretch-activated channels.

Polyvalent Cation Effects on Gating at Negative Potentials

hCx37 hemichannels were closed at potentials between −100 and +10 mV when divalent cations were added to the bathing solution (Fig. 1) and linear with respect to voltage when there were no divalent cations in the bath (Fig. 2). We, therefore, first examined the concentration dependence of divalents over this potential range. Fig. 3 A shows hCx37 currents before (left), during treatment with (middle), and after wash-out of (right) 1 mM Ca^{2+}. Addition of Ca^{2+} to the bath reduced current (Fig. 3 A and D, circles) and shifted the zero-current potential of each oocyte to a more negative potential. Rather than having a reversal potential of −13 mV, the oocytes regained a reversal potential of −40 mV, precisely where the endogenous conductances reversed in control oocytes (Fig. 2 C and Fig. 3 E). The effects of Ca^{2+} on current magnitude and reversal potential were completely reversible upon wash-out of the ion (Fig. 3 A and D, triangles), suggesting

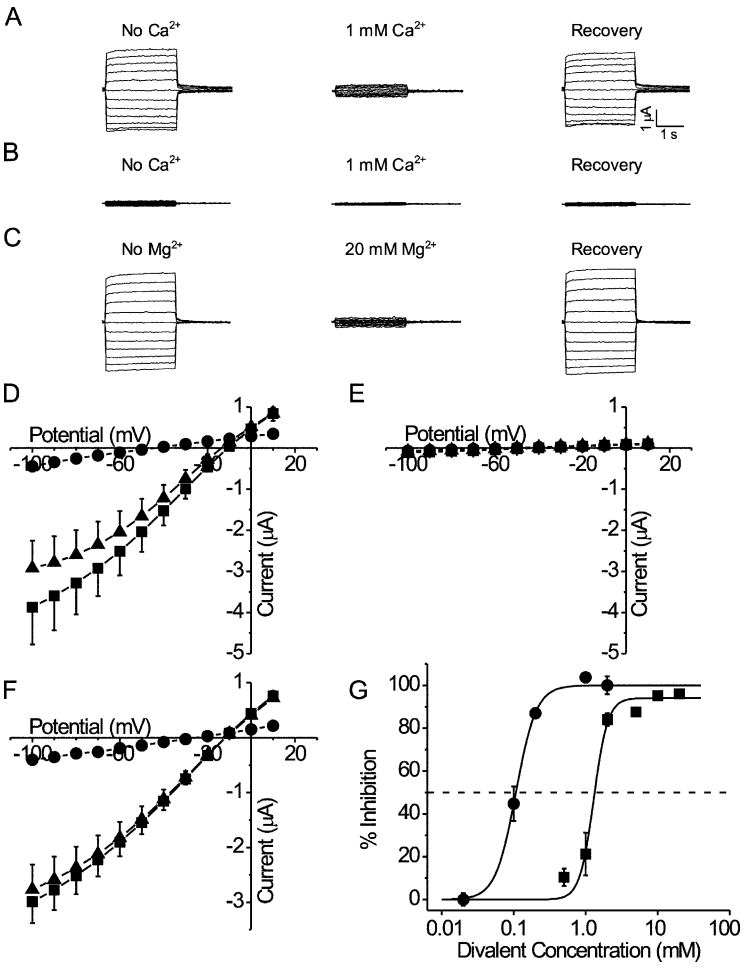

FIGURE 3. hCx37 hemichannel currents are reversibly inhibited by divalent cations. Representative currents resulting from a series of voltage steps from a holding potential of −40 mV to potentials ranging from −100 to +10 mV in 10-mV increments for oocytes injected with hCx37 RNA along with AntiCx38 (A and C) and an oocyte injected only with AntiCx38 (B). (A) Currents from hCx37 hemichannels before (left), during treatment with (middle), and after wash-out of (right) 1 mM Ca^{2+}. (B) Currents from an oocyte injected only with AntiCx38 before (left), during treatment with (middle), and after wash-out of (right) 1 mM Ca^{2+}. (C) Currents from hCx37 hemichannels before (left), during treatment with (middle), and after wash-out of (right) 20 mM Mg^{2+}. (D) Average, isochronal current–voltage relationships for oocytes injected with hCx37 RNA plus AntiCx38 and stored in 0DivOR2. Recordings were made before (■, $n = 8$), during treatment with (●, $n = 8$), and after wash-out of (▲, $n = 8$) 1 mM Ca^{2+}. (E) Average, isochronal current–voltage relationships for oocytes injected with AntiCx38 alone and stored in 0DivOR2. Recordings were made before (■, $n = 3$), during treatment with (●, $n = 3$), and after wash-out of (▲, $n = 3$) 1 mM Ca^{2+}. (F) Average, isochronal current–voltage relationships for oocytes injected with hCx37 RNA plus AntiCx38 and stored in 0DivOR2. Recordings were made before (■, $n = 6$), during treatment with (●, $n = 6$), and after wash-out of (▲, $n = 6$) 20 mM Mg^{2+}. (G) Concentration–response curves (see MATERIALS AND METHODS) showing inhibition of hCx37 hemichannel current at −40 mV as a function of [Ca^{2+}] (●) and [Mg^{2+}] (■). The IC_{50} for Ca^{2+} was 107 μM with a Hill coefficient of 3.1 ± 0.5 (20 μM, $n = 3$; 100 μM, $n = 3$; 200 μM, $n = 5$; 1 mM, $n = 4$; 2 mM, $n = 6$). The IC_{50} for Mg^{2+} was 1.30 mM with a Hill coefficient of 4.5 ± 1.1 (500 μM, $n = 5$; 1 mM, $n = 6$; 2 mM, $n = 4$; 5 mM, $n = 3$; 10 mM, $n = 5$; 20 mM, $n = 4$).

that divalent effects were specific for hCx37 hemichannels and not a nonspecific toxicity affecting the oocyte. Also, the ion did not act on endogenous currents to reduce the overall current at negative potential, since 1 mM Ca^{2+} had no effect on the endogenous currents in control oocytes (Fig. 3 B), which remained small and linear with a reversal potential at −40 mV. Fig. 3 E shows the average current–voltage relationships for oocytes injected with AntiCx38 alone and stored in 0DivOR2. These relationships were identical before, during addition of, and after wash-out of 1 mM Ca^{2+}.

Mg^{2+} ions, which have been shown to bind specifically to hCx37 (Banach et al., 2000), affected the current in much the same way as Ca^{2+}. The addition of Mg^{2+} to the bathing solution reversibly inhibited hCx37 hemichannel current (Fig. 3 C). Current magnitude was significantly reduced in the presence of 20 mM Mg^{2+} (Fig. 3 F, circles). The reversal potential for the oocyte was shifted to a more negative potential (−26 mV), as was the case for 1 mM Ca^{2+}. Mg^{2+} ions required higher concentrations than those of Ca^{2+} to inhibit the current, a trend also observed for Cx46 hemichannels (Ebihara and Steiner, 1993; Ebihara et al., 2003) and Cx32 hemichannels (Gomez-Hernandez et al., 2003). Fig. 3 G shows the concentration–response relationship for the inhibition of hCx37 hemichannel current at −40 mV by extracellular Ca^{2+} (circles) and Mg^{2+} (squares) ions. The IC_{50} for Ca^{2+} was 107 μM with a Hill coefficient of 3.1 ± 0.5. The IC_{50} for Mg^{2+} was 1.3 mM with a Hill coefficient of 4.5 ± 1.1. Ca^{2+} also inhibits Cx46 hemichannels with a Hill coefficient greater than one (Pfahnl and Dahl, 1999). Finally, the inhibition by Mg^{2+} was not complete. Even at saturating Mg^{2+} concentrations, the current was only inhibited 94% as well as it was for Ca^{2+}. Current maximally inhibited by Mg^{2+} could be further inhibited by the addition of 2 mM Ca^{2+} (not depicted), and 20 mM Mg^{2+} (Fig. 3 F) did not shift the reversal potential of the oocytes to the same degree as 1 mM Ca^{2+}. There are two possible explanations for the lack of complete inhibition. The first is that there was a population of channels that remained unblocked. An alternate explanation is that Mg^{2+}, with its smaller radius (0.65 Å versus 0.99 Å for Ca^{2+}) could not completely inhibit current flow in individual channels, only blocking partially and lowering the unitary conductance as previously reported (Banach et al., 2000). Single

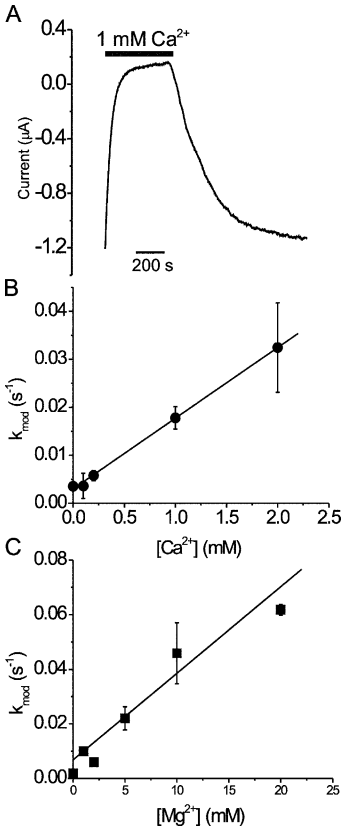

FIGURE 4. The rate of divalent cation inhibition of hCx37 hemichannel currents was concentration dependent. (A) Representative trace showing current from an individual oocyte injected with hCx37 RNA plus AntiCx38. The disappearance of current (left) is upon wash-in of 1 mM Ca^{2+}. The reappearance of current (right) is upon wash-out of Ca^{2+}. These recordings were performed at a holding potential of −40 mV. Both wash-in and wash-out traces were fit with single exponential curves to determine k_{mod}. The time courses were fit with an equation of the form $I = I_\infty - Ae^{-kt}$, where I is the current, I_∞ is the amount of current at steady state, A is the amplitude, t is time, and k is k_{mod} (see RESULTS). The concentration dependence of k_{mod} for hCx37 hemichannel current at −40 mV is shown for Ca^{2+} (B) and Mg^{2+} (C). Both plots were fit with straight lines. For Ca^{2+}, $r = 0.86$; 0 mM, $n = 4$; 0.1 mM, $n = 2$; 0.2 mM, $n = 5$; 1 mM, $n = 5$; 2 mM, $n = 3$. For Mg^{2+}, $r = 0.82$; 0 mM, $n = 2$; 1 mM, $n = 4$; 2 mM, $n = 1$; 5 mM, $n = 4$; 10 mM, $n = 5$, 20 mM, $n = 2$.

channel experiments are necessary to differentiate between these two scenarios.

The differences in affinities for Ca^{2+} and Mg^{2+} could represent differences in the on rate (k_{on}) or the off rate (k_{off}) between the two ions. To distinguish between these two possibilities, the time course of the reduction in hCx37 hemichannel current after addition of divalent cations to the bath was measured by sampling the holding current once per second for 100 ms. The same experiment could be done after removal of divalent cations to determine the time course of recovery from divalent inhibition. Typical examples of these time course experiments can be seen in Fig. 4 A for wash-in (left) and wash-out (right) of 1 mM Ca^{2+} at −40 mV. The time courses were well described by single exponentials with time constants of minutes, which was also observed for Cx46 hemichannel block by 1.8 mM Ca^{2+} (Pfahnl and Dahl, 1999). The Hill coefficients for Ca^{2+} and Mg^{2+} both suggest that multiple ions acted in a cooperative manner to inhibit current in hCx37 (for review see Colquhoun, 1998). The first-order appearance of the time course suggests that, although there were multiple binding steps, the one that was measured must have been much slower than the others, i.e., rate limiting.

Parameters from fits to the time course experiments were used to determine a modification rate constant (k_{mod}). The modification rate is defined by the relationship

$$k_{mod} = k_{on}[M] + k_{off}, \quad (1)$$

where [M] is the concentration of the ion that is inhibiting the current. During the wash-out experiments, [M] was zero, so k_{mod} was equal to k_{off}. The above equation predicts a linear relationship of k_{mod} versus [M]. Fig. 4 (B and C) shows k_{mod} as a function of divalent concentration for Ca^{2+} (B) and Mg^{2+} (C). The data were fit to straight lines, with slopes equal to k_{on} and the Y intercepts equal to k_{off}. Fits gave a predicted value for k_{on} of $0.015 \pm 0.002\ mM^{-1}s^{-1}$ and k_{off} of $0.003 \pm 0.002\ s^{-1}$ for Ca^{2+}. The predicted k_{on} for inhibition by Mg^{2+} was $0.003 \pm 0.0006\ mM^{-1}s^{-1}$ and the predicted k_{off} was $0.007 \pm 0.005\ s^{-1}$. An estimate for the IC_{50} for divalent cation binding was made by dividing k_{off} by k_{on}. This was 200 μM for Ca^{2+}, close to the measured value of 107 μM and 2.3 mM for Mg^{2+}, again close to the measured value of 1.3 mM from the concentration–response curve. Therefore, the kinetic measurements were consistent with the steady-state measurements made for divalent cation inhibition, with an approximately twofold difference in k_{on} and fivefold difference in k_{off} for the two ions accounting for their different affinities for the target.

The trivalent cation Gd^{3+} also inhibited hCx37 hemichannel currents between −100 and +10 mV. Fig. 5 A shows hCx37 hemichannel current before (left) and after (right) the addition of 100 μM Gd^{3+}. Inhibition of current by Gd^{3+}, in contrast to Ca^{2+} and Mg^{2+}, was irreversible. This was presumably due to an extremely low k_{off}. To test this hypothesis, k_{mod} for current inhibition was tested at 100 and 200 μM Gd^{3+}. If k_{off} was close to zero, then k_{mod} should have been equal to $k_{on}[Gd^{3+}]$, according to Eq. 1, and doubling the concentration of Gd^{3+} should double k_{mod}. Fig. 5 B shows the results from this experiment. k_{mod} increased from $0.017 \pm 0.003\ s^{-1}$ in 100 μM Gd^{3+} to $0.042 \pm 0.008\ s^{-1}$ in 200 μM Gd^{3+}, roughly twofold, supporting the conclusion that Gd^{3+} had an immeasurably small k_{off} at negative potentials.

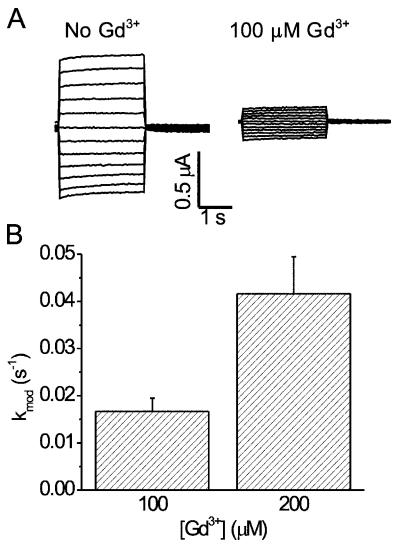

FIGURE 5. Gd^{3+} inhibits hCx37 hemichannel current. (A) Representative currents resulting from a series of steps from a holding potential of −40 mV to potentials ranging from −100 to +10 mV in 10-mV increments for an oocyte injected with hCx37 RNA along with AntiCx38. The currents were recorded before (left) and after (right) the addition of 100 μM Gd^{3+} to the bath. (B) Bar graph showing k_{mod} for hCx37 hemichannel current inhibition by two different concentrations of Gd^{3+}, 100 μM ($n = 4$) and 200 μM ($n = 4$).

Voltage Effects on the Rate of Polyvalent Cation Inhibition

The simplest explanation for the above observations is that hCx37 hemichannels were directly blocked by polyvalent cations. The effect of the applied voltage field on the binding and unbinding rates for polyvalent cations was, therefore, investigated. The time course experiments were performed as above, sampling the current at 1 s intervals as polyvalent cations were washed on while the oocytes were held at various potentials. If these charged particles were blocking within the voltage field or accessing their binding site through the pore, then the rate of modification would be predicted to depend on potential.

The rate of modification of hCx37 hemichannel current by extracellular Ca^{2+} ions was faster at more hyperpolarized potentials (Fig. 6 A, squares), as would be expected for a positively charged ion moving from the outside toward the inside of an oocyte through the voltage field. This effect was solely on the k_{on} since k_{off} was not affected by voltage at the potentials measured (Fig. 6 A, circles). Mg^{2+} behaved similarly (Fig. 6 B, squares). k_{mod} for Mg^{2+} was faster at negative potentials, but k_{off} was not affected by holding potential (Fig. 6 B, circles). The mean k_{off} measured for Ca^{2+} was 0.0035 s^{-1}, very close to the value of 0.003 s^{-1} predicted from the k_{mod} versus concentration curve. The mean k_{off} measured for Mg^{2+} was 0.002 s^{-1}, again reasonably close to the predicted value of 0.007 s^{-1}. k_{mod} for Gd^{3+} was also faster at negative potentials (Fig. 6 C). The effect of holding potential on k_{off} could not be assessed for Gd^{3+} because k_{off} was too small to be measured at these potentials.

k_{on} can be calculated by rearranging Eq. 1. k_{on} for each cation was calculated and plotted as a function of potential (Fig. 6 D). The data were fit with single-exponential decays of the form

$$k_{on} = k_{pos} + Ae^{-V/dV}, \quad (2)$$

where k_{pos} is the minimum k_{on} at more positive potentials, A is the amplitude, V is voltage, and dV is the number of millivolts necessary to change k_{on} by a factor of e. A monovalent cation traveling all the way through the voltage field would undergo an e-fold change in binding rate for every 24 mV. A divalent cation, which feels the field twice as strongly, would be expected to undergo an e-fold change in rate for every 12 mV, and a trivalent every 8 mV. From the fits, it was determined that inhibition by Ca^{2+} changed e-fold for every 11.5 ± 2.7 mV. Therefore, Ca^{2+} permeated the entire way from the outside of the voltage field to the inside. Although electrical distance cannot unequivocally be translated to physical distance, it is likely that the binding site for Ca^{2+} is near the cytoplasmic vestibule. The k_{on} for Mg^{2+} changed e-fold for every 12.8 ± 3.8 mV, which suggests that Mg^{2+} likely bound at the same location as Ca^{2+}. The k_{on} for Gd^{3+} underwent an e-fold change for every 8.0 ± 3.6 mV, the voltage dependence expected for a trivalent that went all the way through the voltage field, suggesting that Gd^{3+} binds to the same location as the divalent cations.

There are two possible explanations for the above observations. The first is that polyvalent cations, albeit slowly, directly blocked the hCx37 hemichannels in a voltage-dependent fashion. Alternatively, polyvalent binding may have been merely permissive of a voltage-dependent transition intrinsic to the channel protein. However, an intrinsic transition in the channel should have had the same voltage dependence regardless of which ion was causing the gating. The observation that the voltage dependence of channel closure was proportionately stronger with the trivalent cation Gd^{3+} than with either divalent cation tested, therefore, suggests that the field was acting directly on the ion to induce channel closure, and not on the channel protein. This is supportive of a role for polyvalent cations as direct blockers of hCx37 hemichannels.

Polyvalent Cation-dependent Voltage Gating at Positive Potentials

In contrast to negative potentials, where the voltage field acted on polyvalent cations to drive them to their binding site, at positive potentials, hCx37 hemichannels passed current, even in the presence of concentra-

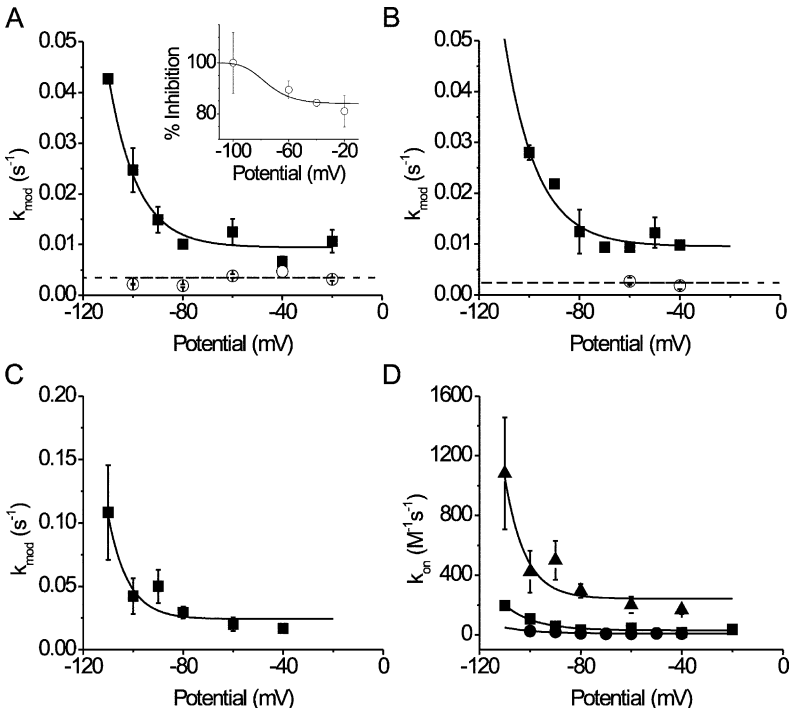

FIGURE 6. Polyvalent cation inhibition of hCx37 hemichannels is voltage dependent. (A) Plot of k_{mod} for hCx37 hemichannel current inhibition by 200 μM Ca^{2+} as a function of potential (■; −110 mV, n = 1; −100 mV, n = 4; −90 mV, n = 3; −80 mV, n = 4; −60 mV, n = 5; −40 mV, n = 4; −20 mV, n = 4). The curve is a single exponential decay fit to the data of the form $k_{mod} = k_{pos} + Ae^{-V/dV}$, where k_{pos} is the minimum k_{mod} at more positive potentials, A is the amplitude, V is voltage, an dV is the amount in millivolts necessary to change k_{mod} by a factor of e. The open circles (○) represent k_{off} as a function of potential (−100 mV, n = 2; −80 mV, n = 3; −60 mV, n = 6; −40 mV, n = 5; −20 mV, n = 3). The straight line shows the mean k_{off} of 0.0035 s^{-1}. The inset shows a plot of the percent inhibition by 200 μM Ca^{2+} as a function of holding potential (−100 mV, n = 4; −60 mV, n = 4; −40 mV, n = 5; −20 mV, n = 3). The curve in the inset represents the predicted percentage block as a function of potential, based on a model of voltage-dependent block for which steady-state block (ssblock) is given by the equation $ssblock = 100/(1 + 10^{((\log(IC50) - \log[Ca])*p)})$, where IC_{50} is predicted by the fits to the measured k_{on} and k_{off} as a function of potential (A, C, and D) and p is the Hill coefficient for Ca^{2+} binding (∼3.1). Data from the inset were leak corrected by the mean of the AntiCx38-injected oocytes from the day each data point was acquired (n = 2–4). The data were normalized to block at −100 mV where close to 100% block is predicted by the above equation for 200 μM Ca^{2+}. (B) Plot of k_{mod} for hCx37 hemichannel current inhibition by 1 mM Mg^{2+} as a function of potential (■; −100 mV, n = 2; −90 mV, n = 1; −80 mV, n = 2; −70 mV, n = 1; −60 mV, n = 4; −50 mV, n = 2; −40 mV, n = 9). The curve is a single exponential decay fit to the data of the form shown in A. The open circles (○) represent k_{off} as a function of potential (−60 mV, n = 4; −40 mV, n = 2). The straight line shows the mean k_{off} of 0.0024 s^{-1}. (C) Plot of k_{mod} for hCx37 hemichannel current inhibition by 100 μM Gd^{3+} as a function of potential (−110 mV, n = 2; −100 mV, n = 7; −90 mV, n = 3; −80 mV, n = 5; −60 mV, n = 3; −40 mV, n = 4). The curve is a single exponential decay fit to the data of the form shown in A. (D) Plot of k_{on} for Ca^{2+} (■), Mg^{2+} (●), and Gd^{3+} (▲) ions as a function of holding potential. The curves are single exponential decays fit to the data of the form $k_{on} = k_{pos} + Ae^{-V/dV}$ (see RESULTS).

tions of Ca^{2+} that completely inhibited current at negative potentials (Fig. 1). We considered whether this behavior represented a symmetrical property of polyvalent cation block, i.e., the field acted on the Ca^{2+} ions at positive potentials to drive them out of the pore. If this were the case, it makes several strong predictions; among them that changes in the polyvalent cation content of the bathing solution should affect macroscopic hCx37 hemichannel gating at positive potentials in a species- and concentration-dependent manner.

Fig. 7 A shows hCx37 currents in response to voltage steps as in Fig. 1 A recorded in 0DivOR2 in the presence of 1 mM Ca^{2+} (left) or 200 μM Gd^{3+} (right). Visual inspection of the currents reveals drastically slower kinetics in the presence of Gd^{3+} compared with the currents measured in Ca^{2+}. Current traces like those in Fig. 7 A were fit with double exponentials of the form

$$I = I_o + A_1(1 - e^{-t*kfast}) + A_2(1 - e^{-t*kslow}), \qquad (3)$$

where I is current, I_o is the offset, A_1 and A_2 are the amplitudes, t is time, and k_{fast} and k_{slow} are the fast and slow rate constants of activation, respectively. This time course was similar to gap junctional currents of hCx37 (Ramanan et al., 1999), which also were well described by two time constants of similar magnitude to those measured in hemichannels. Fig. 7 (B and C) shows the fast and slow rate constants, respectively, for activation of hCx37 hemichannel current with 1 mM Ca^{2+} (circles) and 200 μM Gd^{3+} (squares) in the bathing solution as functions of voltage. Both rate constants were voltage dependent, increasing at greater depolarizations, but the kinetics were much faster in Ca^{2+} at almost all of the potentials studied. This difference was not the result of differences in contamination from the slow, endogenous Na^+ current under the two ionic conditions as the connexin current was much faster in the presence of Ca^{2+} than Gd^{3+}, even at potentials where the contribution of endogenous Na^+ current was negligible (e.g., at E_{Na}). The difference in kinetics was also not accounted for by the difference in the concentration dependence of the effects of Ca^{2+} and Gd^{3+}, since twofold changes in the concentrations of Ca^{2+} (Fig. 7 D) or Gd^{3+} (Fig. 7 E) did not affect the activation kinetics.

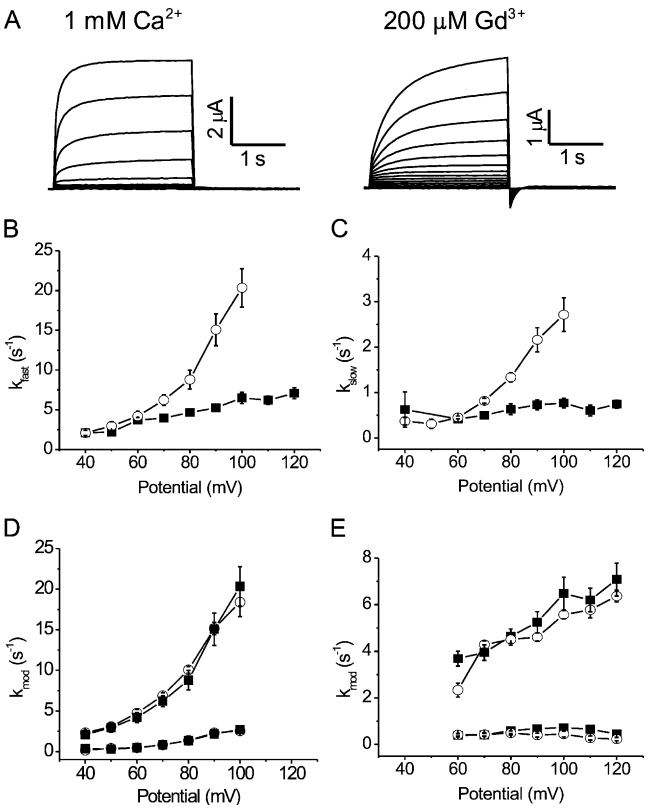

FIGURE 7. Activation rate of hemichannel current depends on the ions in the bathing solution. (A) Currents resulting from a series of voltage steps from a holding potential of −40 mV in 10-mV increments to a potential of +90 mV applied to oocytes injected with hCx37 RNA plus AntiCx38, recorded in 0DivOR2 plus 1 mM Ca^{2+} (left) or 200 μM Gd^{3+} (right). These currents were fit with the sum of two exponentials to determine rate constants (see RESULTS). (B) Fast activation rate constant (k_{fast}) as a function of potential for hCx37-expressing oocytes recorded in 0DivOR2 containing 1 mM Ca^{2+} (○; +40 mV, $n = 8$; +50 mV, $n = 8$; +60 mV, $n = 8$; +70 mV, $n = 9$; +80 mV, $n = 8$; +90 mV, $n = 8$; +100 mV, $n = 8$) or 200 μM Gd^{3+} (■; +60 mV, $n = 15$; +70 mV, $n = 16$; +80 mV, $n = 16$; +90 mV, $n = 16$; +100 mV, $n = 10$). (C) Slow activation rate constant (k_{slow}) as a function of potential for hCx37-expressing oocytes recorded in 0DivOR2 containing 1 mM Ca^{2+} (○; +40 mV, $n = 3$; +50 mV, $n = 7$; +60 mV, $n = 6$; +70 mV, $n = 7$; +80 mV, $n = 7$; +90 mV, $n = 8$; +100 mV, $n = 8$) or 200 μM Gd^{3+} (■; +60 mV, $n = 15$; +70 mV, $n = 16$; +80 mV, $n = 16$; +90 mV, $n = 16$; +100 mV, $n = 10$). (D) k_{fast} (upper) and k_{slow} (lower) for hCx37 hemichannel current recorded in 0DivOR2 containing 1 mM Ca^{2+} (○) or 0.5 mM Ca^{2+} (▲). For k_{fast} in 0.5 mM Ca^{2+}, at +40 mV, $n = 10$; +50 mV, $n = 9$; +60 mV, $n = 10$; +70 mV, $n = 10$; +80 mV, $n = 10$; +90 mV, $n = 9$; and +100 mV, $n = 10$. For k_{slow} in 0.5 mM Ca^{2+}, at +40 mV, $n = 1$; +50 mV, $n = 6$; +60 mV, $n = 10$; +70 mV, $n = 10$; +80 mV, $n = 10$; +90 mV, $n = 10$; and +100 mV, $n = 10$. (E) k_{fast} (upper) and k_{slow} (lower) for hCx37 hemichannel current recorded in 0DivOR2 containing 200 μM Gd^{3+} (■) or 100 μM Gd^{3+} (○). For k_{fast} in 100 μM Gd^{3+} at +60 mV, $n = 5$; +70 mV, $n = 6$; +80 mV, $n = 6$; +90 mV, $n = 6$; and +100 mV, $n = 6$. For k_{slow} in 100 μM Gd^{3+} at +60 mV, $n = 2$; +70 mV, $n = 6$; +80 mV, $n = 6$; +90 mV, $n = 6$; and +100 mV, $n = 5$.

A change in affinity for polyvalents at positive potentials, allowing polyvalent cation dissociation and current flow, is one possible explanation for the activation of current at positive potentials, with the rate of appearance of current dependent on $k_{on}[M]$ and k_{off}. An intracellular polyvalent binding site predicts the opposite behavior for k_{on} and k_{off} at negative and positive potentials. At negative potentials, k_{on} was voltage dependent because the voltage field favored cation entry into the cell and polyvalent cations were driven down their electrochemical gradient to their binding site through the pore and the field. Polyvalent dissociation at negative potentials was voltage independent because, again, the field biased cation flow into the cell and so polyvalents almost exclusively dissociated into the cytoplasm. The opposite would be expected at positive potentials, i.e., k_{off} would be voltage dependent because the voltage field would favor cation exit from the cell and so polyvalents would dissociate and exit through the pore and the field. Conversely, any binding of polyvalents to the site (k_{on}) would be from the cytoplasm and, because of the location of the binding site at the intracellular edge of the electrical field, be expected not to be affected by voltage.

Fig. 7 D shows the fast and slow rate constants for hCx37 hemichannel gating in 0DivOR2 plus 0.5 mM (circles) and 1 mM (squares) Ca^{2+} as a function of potential. There were no differences in either rate constant measured at these two concentrations, as would be expected if $k_{on}[M]$ were very small at positive potentials. For Gd^{3+} as well, doubling the concentration from 100 to 200 μM had no effect on the kinetics (Fig. 7 E). Therefore, we suggest that the time course of current activation at positive potentials primarily reflected the voltage-dependent dissociation of polyvalent cations from their binding site, leaving the channel in a state permissive to current flow. k_{off} for Gd^{3+}, which was immeasurably slow at negative potentials, was also slower than for Ca^{2+} at positive potentials.

If k_{off} was so much greater than k_{on} that polyvalent cation association was not appreciable, current would be expected to increase with time until virtually all polyvalent cations dissociated from all hCx37 channels in the oocyte. Indeed, although hemichannel currents usually reached a plateau value within a few seconds (Fig. 7), when depolarizations were prolonged, currents first reached a pseudo steady-state (as in Fig.7) but later increased and failed to reach a saturating level. In one oocyte, long enough depolarizations were used that current saturation was eventually achieved at ~240 s (unpublished data). Typical examples of currents elicited by long depolarizations are shown in the insets in Fig. 8 (A and C). Such currents are actually common in the literature for other connexins (e.g., Ebihara and Steiner, 1993; Ebihara, 1996). The com-

plex kinetics seen in our records are similar to those reported for certain mutated Cx32 hemichannels (Gomez-Hernandez et al., 2003). This complex current behavior was not due to the activation of endogenous oocyte currents. A developing, outward current was seen in oocytes injected only with AntiCx38 during 40-s depolarizations to +90 mV, however, this current was much smaller than those from hCx37 hemichannels, reaching an average magnitude of 1.3 μA (n = 3; unpublished data), and was likely the result of endogenous Na^+ current, which reverses around +90 mV (Fig. 1 B) and increases slowly over time (Baud and Kado, 1984), or endogenous Cx38 that was not completely eliminated by the antisense.

One major discrepancy remains in reconciling the blocking data obtained in wash-in and wash-out experiments performed at negative potentials with the gating observed in the presence of extracellular polyvalent cations. Specifically, although the time courses of the tail currents when the oocytes were repolarized to −40 mV were slower in the presence of Gd^{3+} than in Ca^{2+} (Fig. 7 A), both tails were very rapid (time constant of tens of milliseconds) compared with the rates measured from the time course of polyvalent cation inhibition of hCx37 hemichannels (time constants of minutes) in wash-in experiments (Figs. 4 and 5). At first glance, it seems almost impossible that channel closure during the wash-in experiments could be the same process as channel closure upon repolarization. One possible factor that could explain such a difference in time course would be the presence of accessory binding sites for polyvalent cations within or near the channel pore. This is not unreasonable to consider since current kinetics were complex under some experimental conditions (Fig. 8, A and C, insets). Binding to such sites would increase the concentration of polyvalent cations in the vicinity, while still permitting flux of ions through the pore. A time constant for deactivation of ∼0.25 s would require a local concentration of 250 mM Ca^{2+}, calculated from the k_{on} value for the slow binding step at −40 mV (15.9 $M^{-1}s^{-1}$). Assuming a cylindrical pore with a diameter of 30 Å and a pore length of 60 Å, which can hold ∼1,400 water molecules, only six Ca^{2+} ions would be required in the vicinity to maintain such a high local concentration.

If a local concentration of Ca^{2+} ions were responsible for the rapid decay kinetics measured upon repolarization to −40 mV, it makes a testable prediction that longer depolarizations would favor fewer polyvalent cations in the vicinity and the tail current would be slower. The inset in Fig. 8 A shows currents resulting from depolarizing pulses to +90 mV of increasing durations (5, 10, 20, and 40 s) in 0DivOR2 plus 0.5 mM Ca^{2+}. Consistent with the prediction, tail currents were markedly prolonged after longer depolarizations. Tails

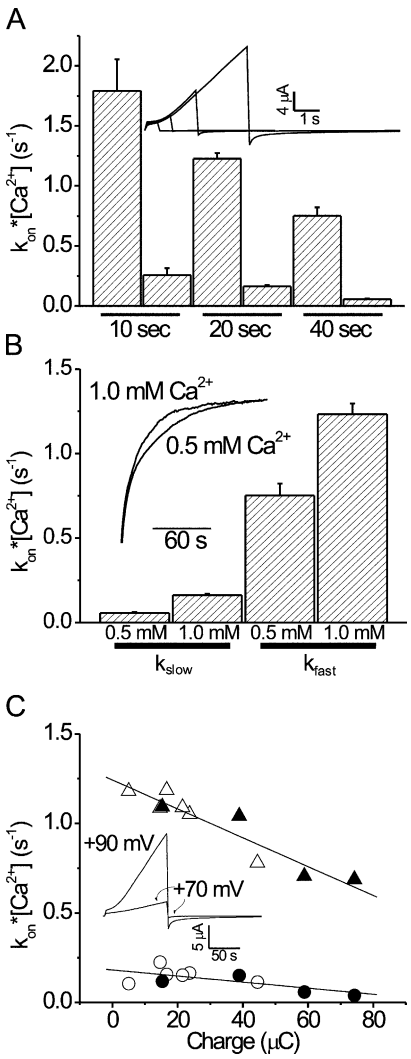

FIGURE 8. Current deactivation depends on polyvalent concentration and flux during channel opening. (A) Fast and slow rate constants of deactivation in 0.5 mM Ca^{2+} as a function of the length of the depolarizing pulse to +90 mV. At 10 s, n = 10, at 20 s, n = 9, and at 40 s, n = 6. The inset shows representative current traces that are the response to depolarization for 5, 10, 20, and 40 s to +90 mV from a holding potential of −40 mV, followed by repolarization to −40 mV. (B) Fast and slow rate constants of deactivation at −40 mV following 40-s depolarizing pulses to +90 mV as a function of extracellular Ca^{2+} concentration. The inset shows representative tail currents recorded upon repolarization to −40 mV in 0DivOR2 plus 1.0 mM Ca^{2+} and 0.5 mM Ca^{2+}. For 0.5 mM Ca^{2+}, n = 6; for 1.0 mM Ca^{2+}, n = 9. (C) Fast (triangles) and slow (circles) rate constants for deactivation at −40 mV as a function of the amount of charge passed during 40-s depolarizing pulses to +90 mV (filled symbols) or +70 mV (open symbols). Each data point represents an individual experiment. A total of six oocytes was used to gather the data. The data were fit to straight lines (k_{fast}, r = 0.9; k_{slow}, r = 0.7). The inset shows representative current traces corresponding to depolarization from a holding potential of −40 to +70 mV and +90 mV followed by repolarization to −40 mV in a single oocyte. Data were acquired at a sampling rate of 100 Hz and filtered at 50 Hz. Rate constants were corrected by the k_{off} for Ca^{2+} at negative potentials (0.0035 s^{-1}) to yield a value of k_{on}*[Ca^{2+}].

were best fit as the sum of two exponentials and both rate constants were similarly slowed; data are summarized in Fig. 8 A in the bar graph. Not only were the rate constants slowed, but the slow rate constant following repolarization to −40 mV after 40-s pulses to +90 mV was 0.06 s^{-1}, which approached, i.e., was on the same order of magnitude as, the 0.01 s^{-1} k_{mod} predicted for 0.5 mM Ca^{2+} from the k_{on} and k_{off} measured during the wash-in experiments in which the local concentration of Ca^{2+} would have been near zero. It is, therefore, likely that the slow rate constant of deactivation after long depolarizations is identical to the rate-limiting step for Ca^{2+} inhibition of hCx37 hemichannels measured during the wash-in experiments.

An alternate explanation for these observations is that long times favored intrinsic channel gating to open states that deactivated more slowly. We looked, therefore, for another test to help discriminate between gating that was independent of block/unblock and gating that was block/unblock. Given that the primary ions contributing to flux through the channel under these experimental conditions were monovalent cations, it would not be expected that gating intrinsic to the channel would be sensitive to small changes in divalent cation concentration. We, therefore, measured tail currents at −40 mV after 40-s depolarizations in 0.5 mM and 1 mM Ca^{2+}. Not only were deactivation rates faster with the higher Ca^{2+} (Fig. 8 B), but the rate constants were roughly double, as would be expected if the rate constants reflected the association of Ca^{2+} with a blocking site to inhibit current flow. In the presence of a high local concentration of Ca^{2+} in or near the pore, the Ca^{2+} concentration in the bathing solution would not be predicted to affect blocking kinetics. Consistent with this prediction, the bath concentration of Ca^{2+} only affected the blocking kinetics following 40-s depolarizations, which were sufficient to deplete the local concentration.

Concentration and depolarization duration data were consistent with the idea that polyvalent cations empty the channel slowly, probably because of accessory binding sites in or near the channel that do not inhibit monovalent flux. This suggests that flux itself, rather than voltage, would influence the rate of block of current during repolarization. In contrast, intrinsic gating into slowly deactivating open states, independent of block, would be expected to depend on the duration and potential of the depolarization and be independent of the amount of flux through the channel during the depolarizing pulse. To test these possibilities, we compared the rates of deactivation after 40-s depolarizations to two different potentials in oocytes with different magnitude currents. Flux was calculated as the integral of the currents during the depolarizations. Data are shown in Fig. 8 C, where the inset shows example currents for this experiment. Both tail rate constants decreased linearly as a function of flux, independent of whether the depolarizing voltage was +90 or +70 mV. It seems likely, therefore, that the monovalents (mostly K^+ efflux from the oocyte) acted to sweep Ca^{2+} from the pore, lowering the local concentration and thereby slowing the concentration-dependent blocking rate at −40 mV.

DISCUSSION

Model for hCx37 Hemichannel Gating

Our data suggest a model in which voltage-dependent block and relief of block by polyvalent cations, rather than an intrinsic channel gating event, is responsible for the closing and opening of hCx37 hemichannels, similar to the gating of inwardly rectifying K^+ channels (Matsuda et al., 1987; Lopatin et al., 1994) and NMDA receptors (Mayer et al., 1984; Mayer and Westbrook, 1987). The model, shown qualitatively and kinetically in Fig. 9, is similar to models previously proposed for voltage gating of Cx46 hemichannels (Ebihara and Steiner, 1993) and Mg^{2+} block of Cx46 hemichannels (Ebihara et al., 2003), although, unlike our model, those models assume an inherent channel "gate." In our model, the channel is bound to some minimum number (n) of polyvalent cations (M^+) required to occlude current flow, which keep the channel in the fully blocked state (Cx). Upon depolarization, the voltage field favors efflux of polyvalent cations from their intracellular binding site. At least two polyvalent cations must be ejected to allow the channel to enter the unblocked, current flow–permissive, state (Cx*), since the appearance of current was biexponential at positive potentials, and both rate constants depended on the character of the ion in the bathing solution, i.e., currents were slower in the presence of Gd^{3+} than in the presence of Ca^{2+} (Fig. 7). Upon repolarization, the voltage field favors binding of polyvalent cations to the intracellular sites, and current decays with a double exponential time course. This time course reflects blocking of the pore by polyvalent cations, as both rate constants increased approximately twofold when the bathing Ca^{2+} concentration was increased by a factor of two (Fig. 8 B). Block of the channel occurred in tens of milliseconds upon repolarization, consistent with a high local concentration of polyvalent cations, which are likely bound to accessory sites in or near the channel pore. However, sustained depolarization (for tens of seconds) allowed for sufficient flux, primarily of monovalents, through the pore, such that the increased local concentration was depleted, leaving the channel devoid of polyvalent cations (Cx**). Under these conditions, upon repolarization, the rate of current decay, i.e., the rate of polyvalent cation block, was

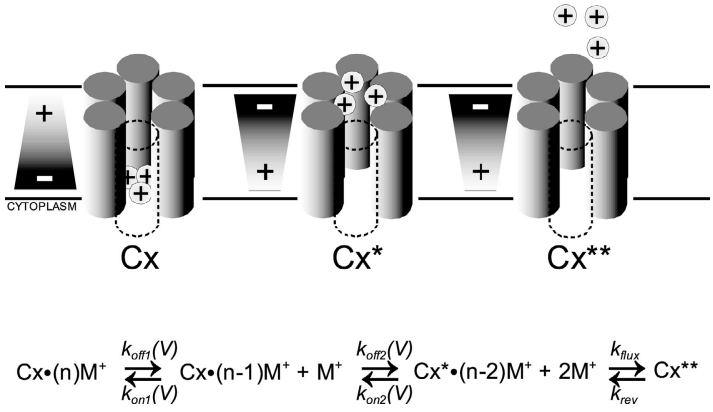

FIGURE 9. Gating model for hCx37 hemichannels. Illustration of the gating process for hCx37 hemichannels. At negative potentials (left) the channel is occupied with several polyvalent cations. These bind to a site on the cytoplasmic side of the channel, blocking current flow. At positive potentials (center) the k_{off} for the polyvalent cations becomes significant, the ions are ejected from the site of block, and current is allowed to flow. Polyvalent cations remain at a high local concentration. Upon extended depolarization (right), the local concentration is depleted as well. Upon repolarization, the polyvalent cations bind the channel again, inhibiting current flow (left). A kinetic model for hCx37 hemichannel gating is shown below. Cx is the blocked hemichannel, Cx* is the unblocked hemichannel, Cx** is the unblocked hemichannel free of any polyvalent cations, M^+ is a polyvalent cation, n is the minimum number of polyvalent cations needed to inhibit current (see DISCUSSION).

much slower (requiring tens of seconds). The slow time course of block approached that seen during wash-in of polyvalent cations to channels that were previously depleted of polyvalent cations by prolonged exposure to polyvalent cation-free solution. During the wash-in experiments, however, both block and recovery followed single-exponential time courses, which suggests that, under these conditions, one, slower blocking event was rate limiting.

Even though block was extremely slow, we have chosen to model the voltage gating of this channel as a simple block/unblock reaction scheme. Block of channels with narrow pores and single binding sites is usually rapid and complete, producing flickering on the single-channel level. However, hCx37 hemichannels have much larger pores and block likely requires multiple ions. Therefore, the details of concentrating and mixing of ions in the local environment of the channel pore as well as the interaction of the multiple ions necessary to inhibit the channel are likely to be very complex. While this complexity cannot be fully appreciated in macroscopic current measurements, the kinetics measured provide a convenient handle for understanding this interesting phenomenon. Single channel and mutational experiments should supply the necessary details for understanding this process in its entirety.

Polyvalent cation effects were the result of specific binding to a site on hCx37, i.e., their effects could not be explained by surface charge screening alone. There are three reasons for this conclusion. First, the macroscopic current–voltage relationship for hCx37 in the presence of high concentrations of polyvalent cations was not affected by doubling the concentration of the bathing polyvalent cation (not depicted) nor were the kinetics of current activation (Fig. 7, D and E). Second, widely different concentrations of Mg^{2+} and Ca^{2+} were required to have the same effect on closure of hCx37 hemichannels (Fig. 3 G). A pure surface charge screening effect, i.e., with no binding, predicts that divalent cations should act equally, so this disparity in the concentration dependence of divalent effects on the current indicates specific binding to the channel. Finally, a pure surface charge screening would produce its effect on the current–voltage relationship by shifting gating to more depolarized potentials as illustrated in the simulations in Fig. 10 A. Upon removal of polyvalent cations, lack of surface charge screening would shift gating in the hyperpolarized direction. If gating were shifted far enough, as in the bold curve labeled number 1, the conductance would have been maximal over the voltage range tested, which would have resulted in a linear current–voltage relationship like the one labeled number 1 in the inset of Fig. 10 A and like that seen experimentally in Fig. 2 C. However, surface charge screening effects also predict that maximal conductance would not be reduced by intermediate concentrations of divalent cations, i.e., gating would shift but maximum conductance would eventually be achieved, as illustrated in the inset in Fig. 10 A. Fig. 10 B (inset) shows the current–voltage relationships for channels recorded in 0DivOR2 plus 0.02 mM Ca^{2+} (squares), 0.1 mM Ca^{2+} (circles), 0.2 mM Ca^{2+} (triangles), and 1 mM Ca^{2+} (inverted triangles). At concentrations of Ca^{2+} that submaximally inhibited the current (e.g., 0.1 and 0.2 mM) the current–voltage relationships remained linear between −100 and +10 mV (see further discussion of this below) but the slopes were reduced proportional to the external [Ca^{2+}] (Fig. 10 B). Taken together, these argue that polyvalent cations do not affect the channel solely by screening surface charges.

It is the case that the fastest rates measured approached the exchange time of the bath solution (see MATERIALS AND METHODS), which may have led to underestimation of the true values. However, the concentration dependence of the rate of both Ca^{2+} and Mg^{2+} inhibition of hCx37 hemichannels remained linear, even at higher concentrations at which the modifica-

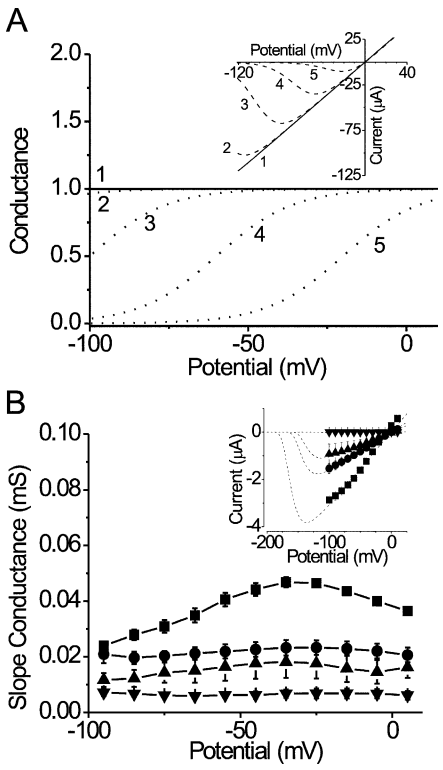

FIGURE 10. Polyvalent cation effects are not due to surface charge screening. (A) Simulated conductance–voltage curves. Each curve is shifted 40 mV relative to the next. Increasing numbers correspond to increasing amounts of polyvalent cations (see DISCUSSION). The inset shows current–voltage relationships corresponding to the conductance–voltage relationships. The bold lines in both the figure and inset correspond to the maximal conductance over the voltage range depicted. (B) Plot of the conductance–voltage relationship for hCx37 in 0DivOR2 plus 0.02 mM Ca^{2+} (■, $n = 6$), 0.1 mM Ca^{2+} (●, $n = 4$), 0.2 mM Ca^{2+} (▲, $n = 6$), and 1 mM Ca^{2+} (▼, $n = 4$). The corresponding, isochronal current–voltage relationships, shown in the inset, represent current responses to the voltage protocol shown in Fig. 2. Conductance was determined at each potential from the slope of the current–voltage relationship between adjacent points. The dashed lines in the inset are predicted currents after 2.5-s voltage pulses based on the expectation from steady-state block in Fig. 6. In brief, the steady-state block was determined for −40 mV, and each new test potential. These values were connected by single exponentials with k_{mod} determined by the measured k_{off} and k_{on} (Fig. 6) and the $[Ca^{2+}]$. The predicted amount of block at 2.5 s was multiplied by an open-channel, current–voltage relationship predicted by a line formed between the current at −40 mV, divided by the fractional block at that potential (Fig. 3 G) and the origin.

tion rates measured were closest to the exchange time (Fig. 4, B and C), and successfully predicted the steady-state EC_{50} measurements, suggesting that even the fastest rates were measured accurately. Additionally, the voltage dependence of the rate of inhibition was also recapitulated in steady-state measurements. The average wash-out rate constants for both Mg^{2+} and Ca^{2+} were much slower (by a factor of >10) than the bath exchange rate constant. Assuming, therefore, that these were reliable measurements, the off-rate constants were small and did not change as a function of voltage at negative potentials. With a k_{on} that changes as a function of potential and a k_{off} that remains constant, one would predict that the IC_{50} for inhibition of hCx37 hemichannels by divalent cations would decrease, leading to an increase in the percentage block as a function of potential. This is shown in the inset of Fig. 6 A. These data were well described by the predictions made by our kinetic data (see the legend for Fig. 6).

Voltage-dependent block by extracellular Ca^{2+} would be expected to produce a nonlinear current–voltage relationship, i.e., a reduction in current at more negative potentials in the presence of Ca^{2+}, as has been observed repeatedly for narrow pores. However, this was not observed for hCx37 hemichannels; current–voltage relationships remained linear over the potential range from −100 to +10 mV, a range over which voltage-dependent block was nonetheless demonstrated in Fig. 6 A (inset). This seeming inconsistency is resolved when one considers the slow time constants involved. Nonlinear current–voltage relationships represent an equilibrium state, but, unlike for divalent block of narrow pores where block occurs almost instantaneously, here the 2.5-s steps used were too short for block to reach steady state. This is illustrated in the inset of Fig. 10 B, which shows the amount of current remaining ~2.5 s after each voltage step was applied to oocytes that were equilibrated in various concentrations of Ca^{2+} at −40 mV and the predictions for current (dashed lines) expected after a 2.5-s voltage pulse, using rate constants derived from Fig. 6. These simulations predict the linear current–voltage relationships we observed over the potential range tested.

The wash-in rate constants for Ca^{2+} (Fig. 6) contrast sharply with the tail current rate constants in the presence of Ca^{2+} (Fig. 8), where the accessory site for polyvalent cation binding was filled. The linearity of the current–voltage relationships in Fig. 10 suggests, therefore, that the accessory site for polyvalent cation binding was not filled, since an increased local $[Ca^{2+}]$ would have greatly increased the rate constants, producing nonlinear current–voltage relationships. It is possible that the accessory site does not fill until the channels are completely blocked or, alternatively, that it is only filled by ions exiting the pore as upon depolarization. Knowledge of the molecular nature of the accessory site will make it possible to test such predictions.

While direct block of hCx37 hemichannels is the simplest explanation for our results, the possibility that a conformational change occurs in the channel following polyvalent cation binding to close the channel cannot be completely excluded. If such a conformational change occurs, however, it must be much faster than the binding, so as not to be detected. Furthermore,

polyvalent cations must be required for this conformational change. Lastly, the voltage sensitivity of the channels must arise from the voltage field acting directly on the ions, rather than the channel protein, given that differences in gating correlated with ion valence and species. Single channel records will be needed to definitively distinguish between these possibilities.

Data in the literature from other hemichannels can be interpreted to suggest an interaction between the voltage field and divalent block. For example, for Cx46, Pfahnl and Dahl (1999) studied the effect of Ca^{2+} on gating of single Cx46 hemichannels. In the absence of added Ca^{2+}, Cx46 hemichannels in excised, outside-out patches opened over a large range of both negative and positive potentials. Upon addition of 5 mM Ca^{2+} to the outside, however, the channels only gated to the open state at positive potentials, as the model predicts. A recent paper by Ebihara et al. (2003) showed that Mg^{2+} can also inhibit Cx46 hemichannels, in a manner consistent with both high and low affinity sites for divalent cation binding. These authors even suggested that divalent cations may be a necessary cofactor for hemichannel voltage gating of Cx46.

If unbinding of polyvalent cations were responsible for the opening of hemichannels, one might expect at least some single channel events to show subconductance states associated with partially unblocked channels. In fact, single Cx46 hemichannel current records (Trexler et al., 1996) exhibited subconductance states briefly visited during channel opening that did not correlate with the major subconductance state visited by the channel following activation. It is possible that such substates correspond to sojourns through partially blocked states during channel opening.

Location of the Polyvalent Binding Site

The voltage dependence of polyvalent cation block predicts the binding site to be on the cytoplasmic side of the channel, based on the Woodhull analysis (Woodhull, 1973). The original model described block in a narrow, single-file pore, in which the blocking ion could not permeate. For Cx channels, the pore is clearly not narrow, multiple ions are required to block, and ions can dissociate and exit the pore in both directions. However, an intracellular location for the polyvalent cation binding site, coupled with the fact that ions can both block and permeate, successfully predicts the behavior for the rates of polyvalent cation binding, with on rates that were voltage dependent at negative potentials (and small and voltage independent at positive potentials) and off rates that were voltage dependent at positive potentials (and small and voltage independent at negative potentials).

Our data indicate the electrical distance for polyvalent cation binding; they do not provide a physical distance or molecular basis for this ion binding. While few acidic residues exist on the cytoplasmic side of the transmembrane domains of hCx37, there are many acidic residues on the NH_2 and COOH termini of the channel, regions previously implicated in voltage gating of other connexins (Revilla et al., 1999; Kumari et al., 2000; Oh et al., 2000; Purnick et al., 2000a,b; Anumonwo et al., 2001), which may play a role in polyvalent cation binding. Further experiments will be required to determine whether these domains are involved in polyvalent cation block. Finally, our data do not rule out the possibility that a molecule like calmodulin that may be closely associated with the protein constitutes the polyvalent binding site. Calmodulin, which is putatively involved in chemical gating of Cx channels (for review see Peracchia, 2004), is activated by Ca^{2+}, Mg^{2+}, and Gd^{3+} (Rainteau et al., 1989).

A recent report (Gomez-Hernandez et al., 2003) showed that mutations in acidic residues on the second extracellular loop of Cx32 hemichannels (D169 and D178) affected their sensitivity to divalent cation block. While mutations at this site altered the concentration dependence of Ca^{2+} regulation, they did not eliminate Ca^{2+} block entirely. Therefore, while it is possible that these negative charges constitute the polyvalent cation blocking site for Cx32, another explanation is that these residues constitute an accessory site for polyvalent binding, like the one we propose for hCx37. The second extracellular loop of hCx37 also has two negative charges with a glutamate (E182) and aspartate (D197), the latter of which is at a position analogous to the D178 residue of Cx32, raising the possibility that these contribute to the accessory binding site, which we observed. Mutations at such a site would be predicted to affect the IC_{50} and kinetics of polyvalent cation effects, as seen in the paper by Gomez-Hernandez et al. (2003), but not eliminate Ca^{2+}or voltage sensitivity entirely. Mutational analysis will be necessary to determine their role in hCx37.

Pfahnl and Dahl (1999) have investigated the location of the Ca^{2+} gate in Cx46 hemichannels. They used the accessibility of a large reagent (MBB), which reacts with free sulfhydryl groups. By creating a cysteine mutant in a pore-lining residue (L35C), they could irreversibly, partially block current, as long as the mutated residue was accessible to MBB. The voltage effects on Ca^{2+} block of Cx46 hemichannels was consistent with Ca^{2+} block at a site within the voltage field, i.e., Ca^{2+} blocked only from the outside at negative potentials and only from the inside at positive potentials. Using MBB, they determined that the Ca^{2+} gate must be extracellular to the cysteine residue at position 35. This may represent a difference in the Ca^{2+} binding location between different channels in the Cx family. On the other hand, it is possible that position 35, whose ex-

act physical location is unknown, is toward the intracellular side of the pore. It must be remembered that only the binding site's electrical distance is predicted here. The physical distance over which the voltage drops is unknown. Finally, we cannot formally exclude the possibility that there is a gating event that occurs in the channel that depends on, but is much faster than, the binding of Ca^{2+}. If this were to occur, then the gate could be at a site distinct from the actual binding site for Ca^{2+}.

As stated before, the exact location of the polyvalent cation binding site in Cx channels may vary from one family member to another. Unlike hCx37 hemichannels, Cx46 hemichannels clearly show a shift in the kinetics of both activation and deactivation with increasing amounts of Ca^{2+} (Ebihara and Steiner, 1993). For hCx37, we ascribe the observation that only deactivation is dependent on the concentration of extracellular Ca^{2+} to a binding site on the intracellular side of the field, which would predict that only filling of the binding site would be favored at negative potentials, while only emptying of the binding site would be favored at positive potentials. Such experimental observations have been reported for hemichannels formed by Cx38, the closest identified orthologue to Cx37 (Ebihara, 1996). If the binding site were not at one extreme end of the voltage field, then the applied voltage would not favor filling or emptying of the binding site at a given potential to the extreme seen for hCx37, and the concentration of Ca^{2+} would be expected to affect activation as well as deactivation rates.

Implications for hCx37 Gap Junction Channel Gating

The question remains: does the gating model for hCx37 hemichannels apply to gap junction channels formed by hCx37 or other connexins? The model predicts that, at rest, hCx37 gap junction channels between two cells at the same potential would be exposed to very low concentrations of Ca^{2+} (10^{-7} M) and concentrations of Mg^{2+} (1–2 mM) that approach the IC_{50} value of 1.3 mM measured for hCx37 hemichannels at −40 mV. It is important to note that filling of the polyvalent cation site from the cytoplasm would not require movement of Mg^{2+} through the voltage field, and, therefore, the IC_{50} value that directly applies to this case would be the IC_{50} at 0 mV. While this was not directly measured, the values for k_{on} and k_{off} were constant over the voltage range between −40 and 0 mV (Fig. 6), so the IC_{50} value would not be expected to change significantly. Therefore, at an intracellular Mg^{2+} concentration of 1.5 mM, ∼60% of the channels would be blocked even at rest. Upon application of a transjunctional voltage, there would be an initial passage of current through the unblocked channels, proportional to the applied voltage step. This would account for the immediate, Ohmic rise in gap junction current upon application of a transjunctional voltage. Two changes would quickly affect the current. On the more positive side of the junction, k_{off} for Mg^{2+} would increase, as would the driving force for cation efflux. On the more negative half of the junction, the k_{on} for Mg^{2+} would increase exponentially as a function of voltage, with no change in k_{off}, causing an increase in affinity for Mg^{2+} and therefore a greater magnitude of block, and current would decrease to a steady-state value. If voltage-dependent block by polyvalent cations were responsible for hCx37 gap junction channel closure in response to a transjunctional voltage difference, the decay rate from the initial current level to steady state would be affected by the concentration of intracellular Mg^{2+}. Ramanan et al. (1999) demonstrated that increasing the intracellular Mg^{2+} from 0.08 mM to 10 mM greatly enhanced the rate of gap junction current decay. Furthermore, the currents were less voltage sensitive in the lower Mg^{2+} concentration, so that larger transjunctional voltages were required to see a reduction in current. Both of these observations are consistent with Mg^{2+} acting as an exogenous gating particle in hCx37 gap junctional channel, since increasing the Mg^{2+} concentration would increase the quantity $k_{on}[Mg^{2+}]$, leading to faster block and therefore faster gating of the channel. Finally, in pairs of cells with asymmetrical Mg^{2+} concentrations, i.e., the cell on one half of the junction contained 0.08 mM Mg^{2+} and the cell on the other half of the junction contained 10 mM Mg^{2+}, the current decayed with a time course that resembled that in 10 mM symmetrical Mg^{2+} when the 10 mM cell was stepped positive and decayed with a time course resembling that in 0.08 mM Mg^{2+} when the cell containing 0.08 mM Mg^{2+} was stepped positive. These results are also consistent with our model, in which the field would act on cations on the positive side of the junction, driving them down their electrical gradient to their binding site.

Other Forms of Gating

Our data suggest that gating of hCx37 hemichannels does not occur in the absence of polyvalent cations. As shown in Fig. 2, the macroscopic currents were linear with respect to voltage under these conditions. The typical hemichannel gating phenotype was restored upon introduction of polyvalent cations to the extracellular medium. The interactions between the voltage field and polyvalent cations are sufficient to explain the behavior of the macroscopic currents. It should, however, be considered that multiple mechanisms of gating have been identified for gap junction channels on the microscopic level (for review see Bukauskas and Verselis, 2004). Single-channel analysis of gap junction channels has identified kinetically distinct, transjunctional volt-

age-sensitive (V_j) gates that affect current: a fast gate, which closes the channels to a subconductance state, and a slow gate, the action of which results in a complete closure. Furthermore, gap junction channels have been demonstrated to be gated by changes in the membrane potential (V_m) and by the actions of a chemical gate, which may also be distinct. While we observed no evidence for multiple gating mechanisms in our macroscopic records, single channel recordings will be necessary to determine whether or not these processes still persist in the absence of polyvalent cations.

Functional Significance

Hemichannels formed by hCx37 have a large predicted single channel conductance and permeability. It is, therefore, crucial for unpaired hemichannels to be closed at rest in order for a cell to maintain proper ionic gradients and cytoplasmic solute concentrations. The high extracellular Ca^{2+} concentration, aided by the resting membrane potential appears to be sufficient to keep hCx37 hemichannels blocked when they are not paired with a hemichannel in an apposing cell membrane. Upon pairing, channels no longer are exposed to high extracellular Ca^{2+} concentrations. Cytoplasmic concentrations of Ca^{2+} are on the order of 100 nM, too low to inhibit the channels. However, intracellular Mg^{2+} on the order of 1–2 mM is enough to inhibit some of the hCx37 gap junction channels while still allowing current flow. Other charged cytoplasmic molecules, such as polyamines, which block Cx40 in a voltage-dependent fashion (Musa and Veenstra, 2003), may affect channels as well. In general, modulators like phosphorylation and pH may also regulate intercellular permeability by altering polyvalent binding. Polyvalent cation block is an efficient solution to the problem of keeping hemichannels closed when unpaired while allowing them to open when they form gap junction channels, making voltage and chemical gating in hCx37 hemichannels and possibly other connexin channels synonymous.

The authors thank Agustin D. Martinez and Ryan W. Dennis for their contributions and Jack W. Kyle and Ian W. Glaaser for helpful discussions.

This work was supported by National Institutes of Health grants HL-45466 (E.C. Beyer), DA-07255 (M.C. Puljung), and NRSA F31NS-42972 (M.C. Puljung).

Olaf S. Andersen served as editor.

Submitted: 21 January 2004
Accepted: 4 October 2004

REFERENCES

Anumonwo, J.M., S.M. Taffet, H. Gu, M. Chanson, A.P. Moreno, and M. Delmar. 2001. The carboxyl terminal domain regulates the unitary conductance and voltage dependence of connexin40 gap junction channels. *Circ. Res.* 88:666–673.

Banach, K., S.V. Ramanan, and P.R. Brink. 2000. The influence of surface charges on the conductance of the human connexin37 gap junction channel. *Biophys. J.* 78:752–760.

Barrio, L.C., T. Suchyna, T. Bargiello, L.X. Xu, R.S. Roginski, M.V. Bennett, and B.J. Nicholson. 1991. Gap junctions formed by connexins 26 and 32 alone and in combination are differently affected by applied voltage. *Proc. Natl. Acad. Sci. USA.* 88:8410–8414.

Baud, C., and R.T. Kado. 1984. Induction and disappearance of excitability in the oocyte of *Xenopus laevis*: a voltage-clamp study. *J. Physiol.* 356:275–289.

Baud, C., R.T. Kado, and K. Marcher. 1982. Sodium channels induced by depolarization of the *Xenopus laevis* oocyte. *Proc. Natl. Acad. Sci. USA.* 79:3188–3192.

Beahm, D.L., and J.E. Hall. 2002. Hemichannel and junctional properties of connexin 50. *Biophys. J.* 82:2016–2031.

Bukauskas, F.F., and V.K. Verselis. 2004. Gap junction channel gating. *Biochim. Biophys. Acta.* 1662:42–60.

Colquhoun, D. 1998. Binding, gating, affinity and efficacy: the interpretation of structure-activity relationships for agonists and of the effects of mutating receptors. *Br. J. Pharmacol.* 125:924–947.

Ebihara, L. 1996. *Xenopus* connexin38 forms hemi-gap-junctional channels in the nonjunctional plasma membrane of *Xenopus* oocytes. *Biophys. J.* 71:742–748.

Ebihara, L., V.M. Berthoud, and E.C. Beyer. 1995. Distinct behavior of connexin56 and connexin46 gap junctional channels can be predicted from the behavior of their hemi-gap-junctional channels. *Biophys. J.* 68:1796–1803.

Ebihara, L., X. Liu, and J.D. Pal. 2003. Effect of external magnesium and calcium on human connexin46 hemichannels. *Biophys. J.* 84:277–286.

Ebihara, L., and E. Steiner. 1993. Properties of a nonjunctional current expressed from a rat connexin46 cDNA in *Xenopus* oocytes. *J. Gen. Physiol.* 102:59–74.

Gomez-Hernandez, J.M., M. De Miguel, B. Larrosa, D. Gonzalez, and L.C. Barrio. 2003. Molecular basis of calcium regulation in connexin-32 hemichannels. *Proc. Natl. Acad. Sci. USA.* 100:16030–16035.

Gupta, V.K., V.M. Berthoud, N. Atal, J.A. Jarillo, L.C. Barrio, and E.C. Beyer. 1994. Bovine connexin44, a lens gap junction protein: molecular cloning, immunologic characterization, and functional expression. *Invest. Ophthalmol. Vis. Sci.* 35:3747–3758.

Harris, A.L. 2001. Emerging issues of connexin channels: biophysics fills the gap. *Q. Rev. Biophys.* 34:325–472.

Imanaga, I., M. Kameyama, and H. Irisawa. 1987. Cell-to-cell diffusion of fluorescent dyes in paired ventricular cells. *Am. J. Physiol.* 252:H223–H232.

Kado, R.T., and C. Baud. 1981. The rise and fall of electrical excitability in the oocyte of *Xenopus laevis*. *J. Physiol. (Paris).* 77:1113–1117.

Kumari, S.S., K. Varadaraj, V. Valiunas, and P.R. Brink. 2001. Site-directed mutations in the transmembrane domain M3 of human connexin37 alter channel conductance and gating. *Biochem. Biophys. Res. Commun.* 280:440–447.

Kumari, S.S., K. Varadaraj, V. Valiunas, S.V. Ramanan, E.A. Christensen, E.C. Beyer, and P.R. Brink. 2000. Functional expression and biophysical properties of polymorphic variants of the human gap junction protein connexin37. *Biochem. Biophys. Res. Commun.* 274:216–224.

Lopatin, A.N., E.N. Makhina, and C.G. Nichols. 1994. Potassium channel block by cytoplasmic polyamines as the mechanism of intrinsic rectification. *Nature.* 372:366–369.

Matsuda, H., A. Saigusa, and H. Irisawa. 1987. Ohmic conductance through the inwardly rectifying K channel and blocking by internal Mg^{2+}. *Nature.* 325:156–159.

Mayer, M.L., and G.L. Westbrook. 1987. Permeation and block of *N*-methyl-D-aspartic acid receptor channels by divalent cations in mouse cultured central neurones. *J. Physiol.* 394:501–527.

Mayer, M.L., G.L. Westbrook, and P.B. Guthrie. 1984. Voltage-dependent block by Mg^{2+} of NMDA responses in spinal cord neurones. *Nature.* 309:261–263.

Musa, H., and R.D. Veenstra. 2003. Voltage-dependent blockade of connexin40 gap junctions by spermine. *Biophys. J.* 84:205–219.

Oh, S., C.K. Abrams, V.K. Verselis, and T.A. Bargiello. 2000. Stoichiometry of transjunctional voltage-gating polarity reversal by a negative charge substitution in the amino terminus of a connexin32 chimera. *J. Gen. Physiol.* 116:13–31.

Paul, D.L., L. Ebihara, L.J. Takemoto, K.I. Swenson, and D.A. Goodenough. 1991. Connexin46, a novel lens gap junction protein, induces voltage-gated currents in nonjunctional plasma membrane of *Xenopus* oocytes. *J. Cell Biol.* 115:1077–1089.

Peracchia, C. 2004. Chemical gating of gap junction channels; roles of calcium, pH and calmodulin. *Biochim. Biophys. Acta.* 1662:61–80.

Pfahnl, A., and G. Dahl. 1999. Gating of cx46 gap junction hemichannels by calcium and voltage. *Pflugers Arch.* 437:345–353.

Pfahnl, A., X.W. Zhou, R. Werner, and G. Dahl. 1997. A chimeric connexin forming gap junction hemichannels. *Pflugers Arch.* 433: 773–779.

Puljung, M.C., V.M. Berthoud, E.C. Beyer, and D.A. Hanck. 2000. Hemichannel behavior of human connexin37 expressed in *Xenopus* oocytes. *Society for Neuroscience Annual Meeting.* 314 (Abstr.).

Puljung, M.C., V.M. Berthoud, E.C. Beyer, and D.A. Hanck. 2001a. Inhibition of human connexin37 hemichannels by extracellular divalent cations. *Biophys. J.* 80:126a (Abstr.).

Puljung, M.C., V.M. Berthoud, E.C. Beyer, and D.A. Hanck. 2001b. Kinetics of divalent cation inhibition of hCx37 hemichannels. *2001 International Gap Junction Conference.* 155 (Abstr.).

Puljung, M.C., V.M. Berthoud, E.C. Beyer, and D.A. Hanck. 2003. Hemichannel properties of hCx37 in transfected cells and *Xenopus* oocytes. *2003 International Gap Junction Conference.* 117 (Abstr.)

Purnick, P.E., D.C. Benjamin, V.K. Verselis, T.A. Bargiello, and T.L. Dowd. 2000a. Structure of the amino terminus of a gap junction protein. *Arch. Biochem. Biophys.* 381:181–190.

Purnick, P.E., S. Oh, C.K. Abrams, V.K. Verselis, and T.A. Bargiello. 2000b. Reversal of the gating polarity of gap junctions by negative charge substitutions in the N-terminus of connexin 32. *Biophys. J.* 79:2403–2415.

Rainteau, D., C. Wolf, and F. Lavialle. 1989. Effects of calcium and calcium analogs on calmodulin: a Fourier transform infrared and electron spin resonance investigation. *Biochim. Biophys. Acta.* 1011:81–87.

Ramanan, S.V., P.R. Brink, K. Varadaraj, E. Peterson, K. Schirrmacher, and K. Banach. 1999. A three-state model for connexin37 gating kinetics. *Biophys. J.* 76:2520–2529.

Reed, K.E., E.M. Westphale, D.M. Larson, H.Z. Wang, R.D. Veenstra, and E.C. Beyer. 1993. Molecular cloning and functional expression of human connexin37, an endothelial cell gap junction protein. *J. Clin. Invest.* 91:997–1004.

Revilla, A., C. Castro, and L.C. Barrio. 1999. Molecular dissection of transjunctional voltage dependence in the connexin-32 and connexin-43 junctions. *Biophys. J.* 77:1374–1383.

Ripps, H., H. Qian, and J. Zakevicius. 2002a. Blockade of an inward sodium current facilitates pharmacological study of hemi-gap-junctional currents in *Xenopus* oocytes. *Biol. Bull.* 203:192–194.

Ripps, H., H. Qian, and J. Zakevicius. 2002b. Pharmacological enhancement of hemi-gap-junctional currents in *Xenopus* oocytes. *J. Neurosci. Methods.* 121:81–92.

Saez, J.C., V.M. Berthoud, M.C. Branes, A.D. Martinez, and E.C. Beyer. 2003. Plasma membrane channels formed by connexins: their regulation and functions. *Physiol. Rev.* 83:1359–1400.

Schwarzmann, G., H. Wiegandt, B. Rose, A. Zimmerman, D. Ben-Haim, and W.R. Loewenstein. 1981. Diameter of the cell-to-cell junctional membrane channels as probed with neutral molecules. *Science.* 213:551–553.

Traub, O., B. Hertlein, M. Kasper, R. Eckert, A. Krisciukaitis, D. Hulser, and K. Willecke. 1998. Characterization of the gap junction protein connexin37 in murine endothelium, respiratory epithelium, and after transfection in human HeLa cells. *Eur. J. Cell Biol.* 77:313–322.

Trexler, E.B., M.V. Bennett, T.A. Bargiello, and V.K. Verselis. 1996. Voltage gating and permeation in a gap junction hemichannel. *Proc. Natl. Acad. Sci. USA.* 93:5836–5841.

Valiunas, V. 2002. Biophysical properties of connexin-45 gap junction hemichannels studied in vertebrate cells. *J. Gen. Physiol.* 119: 147–164.

Veenstra, R.D., H.Z. Wang, E.C. Beyer, S.V. Ramanan, and P.R. Brink. 1994. Connexin37 forms high conductance gap junction channels with subconductance state activity and selective dye and ionic permeabilities. *Biophys. J.* 66:1915–1928.

Weber, W.M. 1999. Endogenous ion channels in oocytes of *Xenopus laevis*: recent developments. *J. Membr. Biol.* 170:1–12.

Willecke, K., R. Heynkes, E. Dahl, R. Stutenkemper, H. Hennemann, S. Jungbluth, T. Suchyna, and B.J. Nicholson. 1991. Mouse connexin37: cloning and functional expression of a gap junction gene highly expressed in lung. *J. Cell Biol.* 114:1049–1057.

Woodhull, A.M. 1973. Ionic blockage of sodium channels in nerve. *J. Gen. Physiol.* 61:687–708.